RL-TR-91-115
In-House Report
April 1991

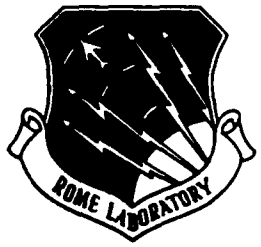

ELECTROMAGNETIC SCATTERING FROM DIELECTRICS -- A TWO-DIMENSIONAL INTEGRAL EQUATION SOLUTION

Marian Silberstein, Capt, USAF

APPROVED FOR PUBLIC RELEASE; DISTRIBUTION UNLIMITED.

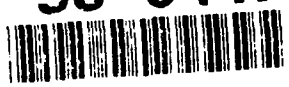

Rome Laboratory
Air Force Systems Command
Griffiss Air Force Base, NY 13441-5700

This report has been reviewed by the Rome Laboratory Public Affairs Division (PA) and is releasable to the National Technical Information Service (NTIS). At NTIS it will be releasable to the general public, including foreign nations.

RL-TR-91-115 has been reviewed and is approved for publication.

APPROVED: Raymond J. Cormier

RAYMOND J. CORMIER
Chief, Applied Electromagnetics Division
Directorate of Electromagnetics

APPROVED: John K. Schindler

JOHN K. SCHINDLER
Director of Electromagnetics

FOR THE COMMANDER. James W. Hyde III

JAMES W. HYDE III
Directorate of Plans & Programs

If your address has changed or if you wish to be removed from the Rome Laboratory mailing list, or if the addressee is no longer employed by your organization, please notify Rome Laboratory (EECT) Hanscom AFB MA 01731-5000. This will assist us in maintaining a current mailing list.

Do not return copies of this report unless contractual obligations or notices on a specific document require that it be returned.

REPORT DOCUMENTATION PAGE

Form Approved
OMB No. 0704-0188

1. AGENCY USE ONLY (Leave blank)	2. REPORT DATE	3. REPORT TYPE AND DATES COVERED
	April 1991	In-House

4. TITLE AND SUBTITLE
Electromagnetic Scattering From Dielectrics - A Two-Dimensional Integral Equation Solution

5. FUNDING NUMBERS
PE-61102F
PR-2305
TA-J4
WU-04

6. AUTHOR(S)
Marian Silberstein, Capt., USAF

7. PERFORMING ORGANIZATION NAME(S) AND ADDRESS(ES)
Rome Laboratory (ERCT)
Hanscom AFB, MA 01731-5000

8. PERFORMING ORGANIZATION REPORT NUMBER
RL-TR-91-115

9. SPONSORING MONITORING AGENCY NAME(S) AND ADDRESS(ES)

10. SPONSORING MONITORING AGENCY REPORT NUMBER

11. SUPPLEMENTARY NOTES
Rome Lab Project Engineer: A.D. Yaghjian/RL/EECT/x3961

12a. DISTRIBUTION AVAILABILITY STATEMENT
Approved for public release; distribution unlimited

12b. DISTRIBUTION CODE

13. ABSTRACT (Maximum 200 words)

An accurate determination of the electromagnetic scattering cross section of many realistic targets must account for their being multi-dimensional and penetrable by the incident EM wave. An existing volume integral equation formulation of EM fields within continuous source regions is well-suited to address this problem. We simply specify the generalized source region of this formulation to be a dielectric body in which currents are induced by the incident wave, and which then "re-radiates" the scattered wave. The relation $E_{tot} = E_{inc} + E_{scat}$ yields a matrix equation to be solved for the unknown currents, which in turn directly determine the scattering cross section. Numerical results are presented for a homogenous, two-dimensional, rectangular target for TE and TM polarizations. The role of the source dyadic term in improving the accuracy of the scattering cross section is investigated both theoretically and numerically.

14. SUBJECT TERMS		15. NUMBER OF PAGES
Scattering Dielectric cylinders	Volume integral equations	34
		16. PRICE CODE

17. SECURITY CLASSIFICATION OF REPORT	18. SECURITY CLASSIFICATION OF THIS PAGE	19. SECURITY CLASSIFICATION OF ABSTRACT	20. LIMITATION OF ABSTRACT
UNCLASSIFIED	UNCLASSIFIED	UNCLASSIFIED	SAR

Contents

Illustrations

Electromagnetic Scattering From Dielectrics – a Two-Dimensional Integral Equation Solution

1. INTRODUCTION

There has been considerable interest throughout the 1970s and 1980s in the scattering of electromagnetic waves from dielectrics, for a wide variety of applications. These include propagation through rain and snow, detection of airborne particulates, coupling of missiles with plasma plumes or dielectric-filled apertures, performance of communications antennas in the presence of dielectric and magnetic inhomogeneities, scattering from birds and other interference in radar systems, microwave hazards to biological (especially human) tissue, hypothermia treatment of cancerous tissues, and last but not least, detection of non-metallic (that is, electrically penetrable) components of military aircraft, missiles, and radar antennas. Numerous papers have addressed mostly differential, but also some integral equation techniques for calculating electromagnetic fields scattered by inhomogeneous dielectric objects. The volume integral equation method is a viable alternative to differential methods, but it has not usually been applied to multi-wavelength objects because of the large matrix inversions required. However, with the recent availability of parallel computers and new matrix-solving algorithms, this limitation is being rapidly overcome.

A further limitation of integral equations concerns the careful treatment of the source region, a controversial issue in the recent past. Originally, this report was intended as a continuation of the source region problem - an application meant to demonstrate a difference

Received for Publication 1 May 1991

when one correctly represents the coincidence of the source and observation points in forming an expression for the scattered electric field. The derivation of the matrix equation presented here and the computer program used for the calculations thus follow directly from previous work on the source region problem.[1]

Upon reviewing the existing literature about scattering from dielectrics, one quickly discovers that in almost every article the primary reference is to Richmond's work of the early 1960s.[2,3] Since Richmond's results match the physical optics approximation results, they have been used as a baseline for comparison in all subsequent work. Surprisingly enough, the theoretical development in this report parallels Richmond's, produced long before the source region controversy emerged. Also, the results of the computer program precisely match Richmond's results for the two-dimensional problem. Since Richmond omits nearly all of the details of his calculation, it is difficult to determine whether he actually did consider the source region, or simply had keen enough physical intuition to choose correct forms of the expressions based on knowledge of their behavior for limiting cases. In this report, the details of the correct closed form integral equation solution are presented explicitly, and the code is available (to DoD workers) as an in-house resource for future modification, if desired.

2. OUTLINE OF THEORY

Figure 1 shows the geometry of a bistatic radar cross section problem. An incident wave excites polarization currents in the dielectric target which then re-radiates the energy in the form of a 'scattered' field. Thus, the target is considered the source of the scattered field, and the standard equation $\mathbf{E}_{scat} = \mathbf{E}_{tot} - \mathbf{E}_{inc}$ is used to calculate this scattered electric field at any point in space. When $\mathbf{E}_{scat}$ is then expressed in terms of the unknown induced polarization current, it quickly yields the scattering cross section, or RCS, used to characterize the target's visibility to radar.

An exact expression for the scattered electric field due to currents induced in a dielectric target has been previously derived, taking care to properly account for the singularity occurring in the electric Green's function when the source and observation points coincide (at $\mathbf{r} = \mathbf{r}'$).

---

[1] Silberstein, Marian (1991) Application of a generalized Leibniz rule for calculating electromagnetic fields within continuous source regions, *Radio Science*, **26** (No. 1):183-190 (a more detailed version is contained in Rome Air Development Center Technical Report 88-333, ADA212470.

[2] Richmond, J.H. (1975) Scattering by a dielectric cylinder of arbitrary cross-section shape, *IEEE Transactions on Antennas and Propagation*, **AP-13**:334.

[3] Richmond, J.H. (1966) TE-wave scattering by a dielectric cylinder of arbitrary cross-section shape, *IEEE Transactions on Antennas and Propagation*, **AP-14**:460.

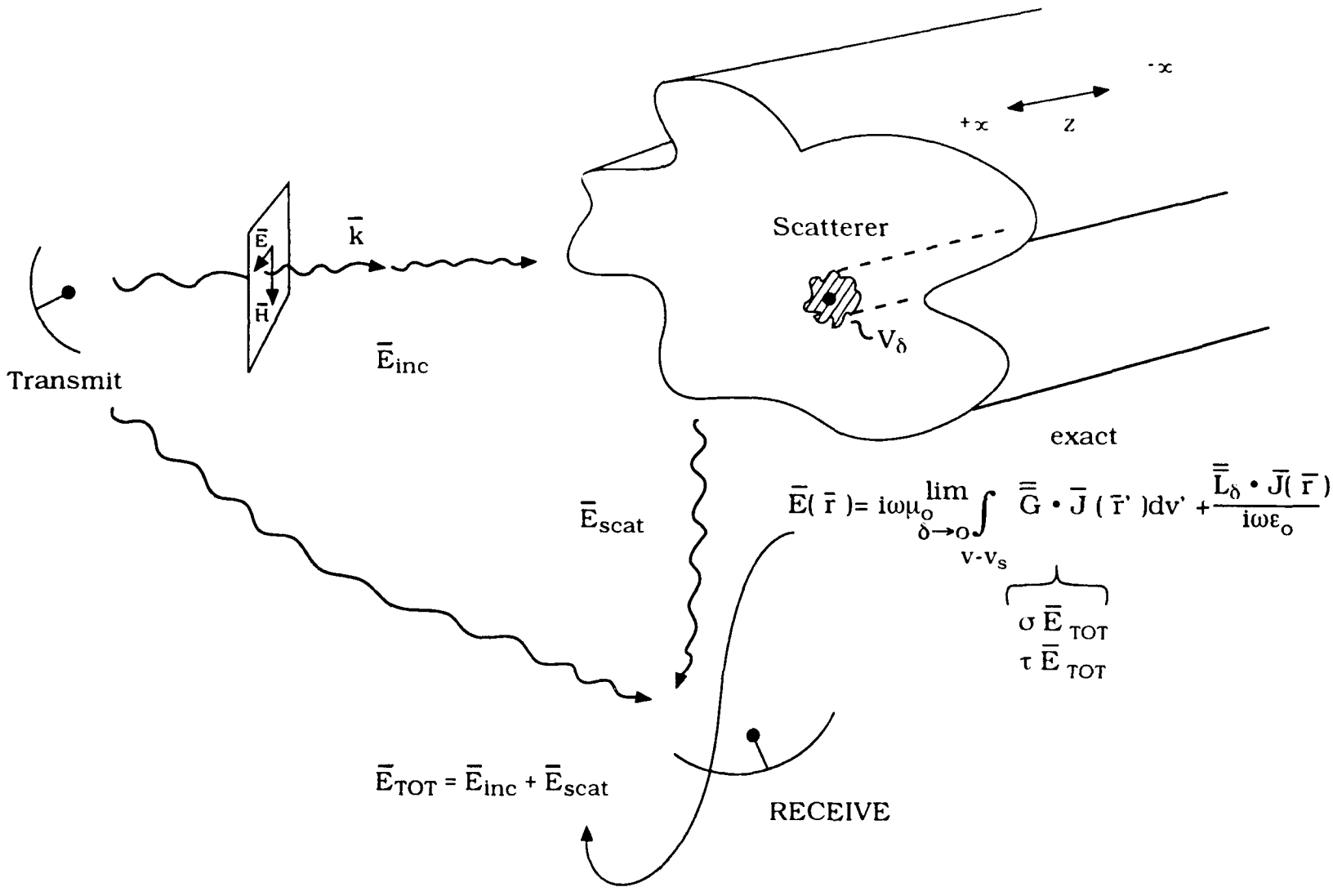

Figure 1. Geometry of a Bistatic Scattering Experiment

$$\mathbf{E}_{scat}(\mathbf{r}) = i\omega\mu_0 \lim_{\delta\to 0} \int_{V-V_\delta} \bar{\mathbf{G}}_E(\mathbf{r},\mathbf{r}') \cdot \mathbf{J}(\mathbf{r}')\, dV' + \frac{\bar{\mathbf{L}}_\delta \cdot \mathbf{J}(\mathbf{r})}{i\omega\varepsilon_0}. \quad (1)$$

This outcome of the controversial "source region problem" contains the important source dyadic, or $\bar{\mathbf{L}}_\delta$, term, accounting for the field contribution at $\mathbf{r} = \mathbf{r}'$. The calculation in this report starts from this expression, and solves the integral equation resulting upon its insertion into the simple scattered field equation above. The reader is urged to review Yaghjian's or Silberstein's development of Eq. (1).[1,4]

The following derivation is performed for a two-dimensional target, that is, an infinite cylinder of arbitrary geometrical cross section. Both TE and TM polarizations are addressed, with plane wave incidence assumed. The three-dimensional problem would proceed in the same manner, but with a simpler Green's function, and is discussed briefly.

3. THEORY FOR TM POLARIZATION

We begin by considering the details of Eq. (1), which can be transformed via the Helmholtz wave equation into the form:

$$\mathbf{E}(\mathbf{r}) = \frac{i}{4\pi\omega\varepsilon_0} \lim_{\delta\to 0} \int_{V-V_\delta} [\nabla'\times\nabla'\times \mathbf{J}(\mathbf{r}')]\psi(\mathbf{r},\mathbf{r}')\, dV' + \frac{\bar{\mathbf{L}}_\delta \cdot \mathbf{J}}{i\omega\varepsilon_0}. \quad (2)$$

Note that the source dyadic term accounts for the contribution to the scattered electric field from the principal volume, V_δ, excluding from the integral the singularity caused at the source point. Also note the dyadic $\bar{\mathbf{L}}_\delta$ varies with the shape of this volume and the fixed position of the singularity within it. Because we have a three-dimensional volume integral equation but wish to investigate a two-dimensional target as the source of the scattered field, we first eliminate the z-dependence by performing the z-integration of the Green's function, and expressing the current and its derivative operators as two-dimensional vectors.[5]

---

[4] Yaghjian, A.D. (1985) Maxwellian and cavity electromagnetic fields within continuous sources, *Am. J. Phys.*, **53**:859.

[5] Yaghjian, A.D. (1980) Electric dyadic Green's functions in the source region, *Proc. IEEE*, **68**:258.

$$\int_{V-V_\delta} \psi(\mathbf{r},\mathbf{r}')\, dV' = \int_{A-A_\delta}\int_{z'=-\infty}^{\infty} \frac{e^{ik|\mathbf{r}-\mathbf{r}'|}}{|\mathbf{r}-\mathbf{r}'|}\, dz'dx'dy'$$

$$= \int_{A-A_\delta} \pi i H_o^{(1)}(k|\mathbf{t}-\mathbf{t}'|)\, dx'dy'.$$

The position vector $\mathbf{r}$ has been replaced by the two-dimensional position vector $\bar{\mathbf{t}} = \hat{x}x + \hat{y}y$, and the principal volume has been replaced by its two-dimensional analog, the cross-sectional principal area A_δ. Substituting this Hankel function expression for ψ in Eq. (2), we have:

$$\mathbf{E}(\mathbf{t}) = \frac{-1}{4\omega\varepsilon_o} \lim_{\delta\to 0}\int_{A-A_\delta} [\nabla_t'\times\nabla_t'\times \mathbf{J}(\mathbf{t}')]\, H_o^{(1)}(k|\mathbf{t}-\mathbf{t}'|)\, dA' + \frac{\bar{\mathbf{L}}_\delta \cdot \mathbf{J}(\mathbf{t})}{i\omega\varepsilon_o}. \tag{3}$$

It is legitimate to move the double curl outside the z'-integration so it only includes y, because the current is constant with respect to z'. The principal volume, of course, is also constant in z'. Thus, the limits are not variable, the z'-integration is continuous, and the derivative operator can be moved in and out of the z' integral sign. From now on we will denote $|\mathbf{t}-\mathbf{t}'|$ as ρ. Using a vector identity, we recast curl (curl $\mathbf{J}$) and write

$$\mathbf{E}(\mathbf{t}) = \frac{-1}{4\omega\varepsilon_o} \lim_{\delta\to 0}\int_{A-A_\delta} \mathbf{J}(\mathbf{t}')\cdot(\nabla_t\nabla_t - \nabla_t^2)\, H_o^{(1)}(k\rho)\, dA' + \frac{\bar{\mathbf{L}}_\delta \cdot \mathbf{J}(\mathbf{t})}{i\omega\varepsilon_o}. \tag{4}$$

With some algebra, we arrive at the two-dimensional scattered field expression

$$\mathbf{E}(\mathbf{t}) = \frac{-k^2}{i\omega\varepsilon_o} \lim_{\delta\to 0}\int_{A-A_\delta} \mathbf{J}(\mathbf{t}')\cdot\bar{\mathbf{g}}_e^o\, dA' + \frac{\bar{\mathbf{I}}_t \cdot \mathbf{J}(\mathbf{t})}{2i\omega\varepsilon_o}, \tag{5}$$

where

$$\bar{\mathbf{g}}_e^o = \frac{i}{4}\left(\frac{\nabla_t\nabla_t}{k^2} + \bar{\mathbf{I}}\right) H_o^{(1)} \tag{6}$$

and

$$\bar{\mathbf{L}}_\delta = \frac{\bar{\mathbf{I}}_t}{2}. \tag{7}$$

We have inserted the value of the source dyadic [Eq. (7)] corresponding to a square principal area because we wish to divide the target into square patches later in the numerical calculation. If a different patch geometry is desired, $\bar{\mathbf{L}}_\delta$ must be adjusted accordingly.[5]

We now consider the two possible polarizations of the incident wave. We begin with the simpler TM polarization, in which $\mathbf{E} = \hat{z}E_z$. For a plane wave, this corresponds to either $\mathbf{E} = \hat{z}e^{ikx}$ or $\mathbf{E} = \hat{z}e^{iky}$. We need only solve the z-component of the equation:

$$\mathbf{E}_z(\mathbf{t}) = \frac{-k^2}{i\omega\varepsilon_o} \lim_{\delta\to 0} \int_{A-A_\delta} (\mathbf{J}(\mathbf{t}') \cdot \bar{\mathbf{g}}_e^o)_z \, dA'. \tag{8}$$

The equation for this polarization is simplified by the vanishing of the source dyadic term. In addition, since the two-dimensional derivative operator has no z-component and the z-component of $\bar{\mathbf{I}}$ is 1, the Green's function is also simplified:

$$(\bar{\mathbf{g}}_e^o)_z = \frac{i}{4} H_o^{(1)}. \tag{9}$$

The equation solved by the FORTRAN program is then

$$\mathbf{E}_{scat\ z}(\mathbf{t}) = \frac{-\omega\mu_o}{4} \lim_{\delta\to 0} \int_{A-A_\delta} H_o^{(1)}(k\rho)\mathbf{J}_z(\mathbf{t}') \, dA'. \tag{10}$$

To evaluate the electric field numerically, we approximate the integral as a summation over the face of the target, divided into N square patches, each with a source point at its center. To exclude the principal area, we initially allow it to occupy an entire square patch, and simply omit the contribution from that patch. The limit occurs as the number of patches increases for a target of fixed size. In Section 5 we improve the accuracy of this treatment to let the principal area approach zero while the square patch size remains fixed, and we then calculate the contribution from the area between these two boundaries. In the meantime,

however, we exclude the singular point by omitting the entire self-cell from the summation as follows:

$$\frac{\Delta A \omega \mu_o}{4} \sum_{i=1}^{N} H_o^{(1)}(k|\mathbf{t}_n - \mathbf{t}_i|)\mathbf{J}_z(\mathbf{t}_i) \; ; \; i \neq n \; . \tag{11}$$

Here, ΔA is the patch area, constant for all patches, and $\mathbf{J_Z}$ is considered constant over the patch, at its center value. Since we want to consider dielectric targets, having only polarization current, we substitute

$$\begin{aligned} \mathbf{J}_{tot} &= \mathbf{J}_{pol} = -i\omega\mathbf{P} \\ &= -i\omega(\varepsilon - \varepsilon_o)\mathbf{E}_{tot} \\ &= \tau\mathbf{E}_{tot}. \end{aligned} \tag{12}$$

Assuming τ is constant over all patches, our scattered field expression then reduces to

$$\frac{\Delta A \omega \mu_o \tau}{4} \sum_{i=1}^{N} H_o^{(1)}(k|\mathbf{t}_n - \mathbf{t}_i|)E_{tot\,z}(\mathbf{t}_i) \; ; \; i \neq n \tag{13}$$

and a summation equation is written as follows for each observation patch, n:

$$\mathbf{E}_{inc\,z}(\mathbf{t}_n) = \mathbf{E}_{tot\,z}(\mathbf{t}_n) + \frac{\Delta A \omega \mu_o \tau}{4} \sum_{i=1}^{N} H_o^{(1)}(k|\mathbf{t}_n - \mathbf{t}_i|)\mathbf{E}_{tot\,z}(\mathbf{t}_i) \; ; \; i \neq n. \tag{14}$$

From a physical viewpoint, if we were to stand at the center point of patch n and measure the field contributions from all the other patches except n we would sense the following contributions:

$$
\begin{aligned}
n=1: \quad \mathbf{E}_{inc\ z}(\mathbf{t}_1) &= \mathbf{E}_{tot\ z}(\mathbf{t}_1) + \frac{\Delta A \omega \mu_o \tau}{4} \left[H_o^{(1)}(k|\mathbf{t}_1 - \mathbf{t}_2|)\mathbf{E}_{tot\ z}(\mathbf{t}_2) \right. \\
&\quad + H_o^{(1)}(k|\mathbf{t}_1 - \mathbf{t}_3|)\mathbf{E}_{tot\ z}(\mathbf{t}_3) \\
&\quad \left. \ldots + H_o^{(1)}(k|\mathbf{t}_1 - \mathbf{t}_N|)\mathbf{E}_{tot\ z}(\mathbf{t}_N) \right] \\
n=2: \quad \mathbf{E}_{inc\ z}(\mathbf{t}_2) &= \mathbf{E}_{tot\ z}(\mathbf{t}_2) + \frac{\Delta A \omega \mu_o \tau}{4} \left[H_o^{(1)}(k|\mathbf{t}_2 - \mathbf{t}_1|)\mathbf{E}_{tot\ z}(\mathbf{t}_1) \right. \\
&\quad + H_o^{(1)}(k|\mathbf{t}_2 - \mathbf{t}_3|)\mathbf{E}_{tot\ z}(\mathbf{t}_3) \\
&\quad \left. \ldots + H_o^{(1)}(k|\mathbf{t}_2 - \mathbf{t}_N|)\mathbf{E}_{tot\ z}(\mathbf{t}_N) \right] .
\end{aligned}
\tag{15}
$$

Clearly, we may substitute unity for the self-cell position (that is, the diagonal matrix element) in our system of equations and we can write it[6] in the form $\mathbf{Ax} = \mathbf{B}$. For convenience, we then multiply Eq. (15) by $4/\Delta A \omega \mu_o$, and replace $\mathbf{E}_{tot}$ by $\mathbf{J}_z/\tau$. The N x N matrix equation appears in the code in terms of J_z, with the constant $4/\Delta A \omega \mu_o \tau$ on the matrix diagonal:

$$
\frac{4}{\Delta A \omega \mu_o} \begin{bmatrix} \uparrow \\ E_{inc_z} \\ \downarrow \end{bmatrix} = \begin{bmatrix} & H_o^{(1)} & \\ \frac{4}{\Delta A \omega \mu_o \tau} & & \\ H_o^{(1)} & & \end{bmatrix} \begin{bmatrix} \uparrow \\ J_z \\ \downarrow \end{bmatrix}
\tag{16}
$$

4. THEORY FOR TE POLARIZATION

The TE incident wave is polarized in the perpendicular direction, so $\mathbf{E} = \hat{x} E_x + \hat{y} E_y$, and the source dyadic does not vanish. In addition, the integral involves coupling between the x-and y-

---

[6] Su, C.C. (1987) Calculation of electromagnetic scattering from a dielectric cylinder using the conjugate gradient method and FFT, *IEEE Transactions on Antennas and Propagation*, **AP-35**:1418.

directions, whereas the TM polarization was completely decoupled. Our scattered field equation is

$$\mathbf{E}_{\text{scat }t}(\mathbf{t}) = i\omega\mu_o \lim_{\delta\to 0}\int_{A-A_\delta} \frac{i}{4}\left(\bar{\mathbf{I}} + \frac{\nabla_t\nabla_t}{k^2}\right)\cdot H_o^{(1)}(k\,|\mathbf{t}-\mathbf{t}'|)\mathbf{J}_t(\mathbf{t}')\ dA' + \frac{\mathbf{J}_t(\mathbf{t})}{2i\omega\varepsilon_o} \tag{17}$$

where the dot product in the integrand, upon manipulation, becomes

$$\left(\bar{\mathbf{I}} + \frac{\nabla_t\nabla_t}{k^2}\right)\cdot H_0^{(1)}(k\,|\mathbf{t}-\mathbf{t}'|)\,\mathbf{J}_t(\mathbf{t}') = \begin{bmatrix} J_x\left(1 + \frac{1}{k^2}\frac{\partial^2}{\partial x^2}\right)H_0^{(1)} + \frac{1}{k^2}J_y\frac{\partial}{\partial x}\frac{\partial}{\partial y}H_0^{(1)} \\ \frac{1}{k^2}J_x\frac{\partial}{\partial y}\frac{\partial}{\partial x}H_0^{(1)} + J_y\left(1 + \frac{1}{k^2}\frac{\partial^2}{\partial y^2}\right)H_0^{(1)} \end{bmatrix}. \tag{18}$$

We refer to the RHS of Eq. (18) as $\mathbf{V}_t$. Substituting the scattered field expression into the standard equation, we have

$$\mathbf{E}_{\text{tot }t}(\mathbf{t}) = \mathbf{E}_{\text{inc }t}(\mathbf{t}) - \frac{\omega\mu_o}{4}\lim_{\Delta A\to 0}\sum_{n=1}^{N}\mathbf{V}_t\,[\rho,\,\mathbf{E}_{t\text{ tot}}(\mathbf{t}')]\,\Delta A_n + \frac{\tau(\mathbf{t})\mathbf{E}_{t\text{ tot}}(\mathbf{t})}{2i\omega\varepsilon_0}. \tag{19}$$

The last term is the source dyadic corresponding to the square principal area, as before. Rearranging, we have

$$\mathbf{E}_{\text{inc }t}(\mathbf{t}_n) = \mathbf{E}_{\text{tot }t}(\mathbf{t}_n)\left[1 - \frac{\tau(\mathbf{t}_n)}{2i\omega\varepsilon_0}\right] + \frac{\omega\mu_o\Delta A}{4}\sum_{i=1}^{N}\mathbf{V}_t\,[\rho,\,\mathbf{E}_{t\text{ tot}}(\mathbf{t}')]\,;\ i\neq n \tag{20}$$

for each of N patches. Again, the stipulation $i \neq n$ excludes the self-patch, where n denotes the patch containing the observation point and i, the patch with the source point. The components of Eq. (20) are:

$$E_{x\,inc}(t_n) = J_x(t_n)\left[\frac{1}{\tau(t_n)} - \frac{1}{2i\omega\varepsilon_0}\right] + \frac{\omega\mu_0\Delta A}{4}\sum_{i=1}^{N} J_x\left(1 + \frac{1}{k^2}\frac{\partial^2}{\partial x^2}H_o^{(1)}\right) + J_y\frac{1}{k^2}\frac{\partial}{\partial x}\frac{\partial}{\partial y}H_o^{(1)}$$

(21)

$$E_{y\,inc}(t_n) = J_y(t_n)\left[\frac{1}{\tau(t_n)} - \frac{1}{2i\omega\varepsilon_0}\right] + \frac{\omega\mu_0\Delta A}{4}\sum_{i=1}^{N} J_y\left(1 + \frac{1}{k^2}\frac{\partial^2}{\partial y^2}H_o^{(1)}\right) + J_x\frac{1}{k^2}\frac{\partial}{\partial x}\frac{\partial}{\partial y}H_o^{(1)}.$$

Note that the argument of the Hankel function is always kρ indicating that each component of the individual electric field induces both components of current, **J** — the reason why the x-and y-components remain coupled. Differentiating the Hankel function, $H_o^{(1)}$, we can express the summation in the $E_{x\,inc}$ equation of Eqs. (21), as:

$$\sum_{i=1}^{N} J_x\left[H_o - \frac{H_1}{k|t_n - t_i|} + \frac{H_2(x_n - x_i)^2}{|t_n - t_i|^2}\right] + J_y\left[H_2\frac{(x_n - x_i)(y_n - y_i)}{|t_n - t_i|^2}\right]. \qquad (22)$$

A similar result occurs for the summation in the $E_{y\,inc}$ equation. If we then write out the summation for a target whose cross-section is divided into N square patches, we obtain this time, a 2N x 2N matrix equation, whereas the TM polarization had only an N x N matrix to invert.

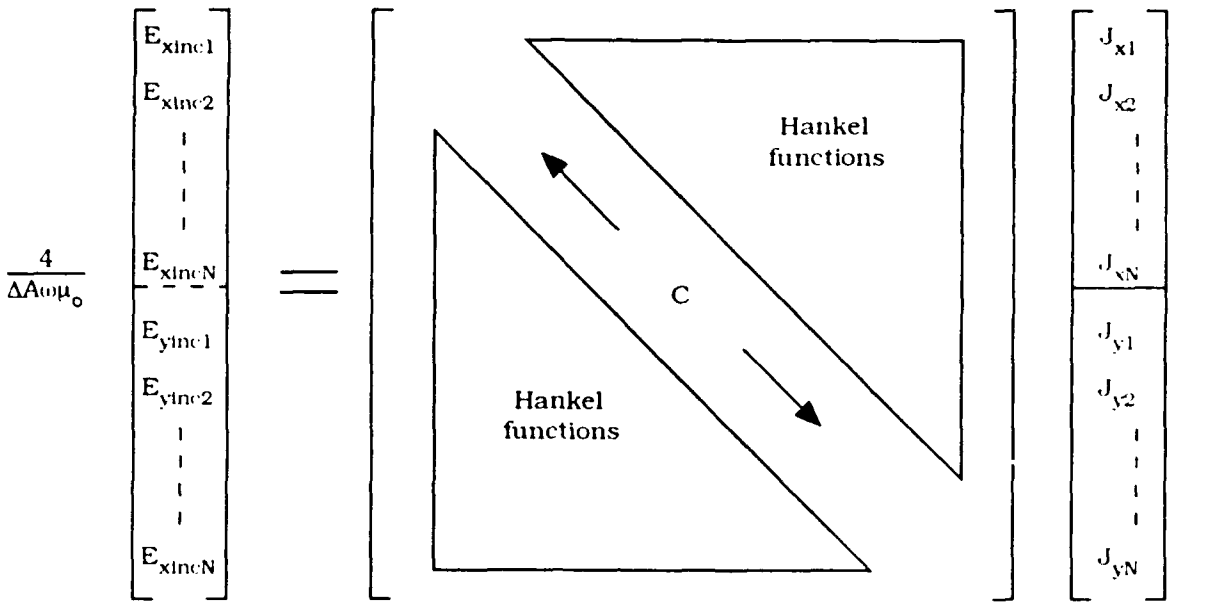

(23)

We do not consider oblique incidence, but only the two cases $\mathbf{E}_{inc} = \hat{y}e^{ikx}$ (vertical target) and $\mathbf{E}_{inc} = \hat{x}e^{iky}$ (horizontal target). The constant C on the matrix diagonal is

$$\left[\frac{1}{\tau} - \frac{1}{2i\omega\varepsilon_o}\right] \frac{4}{\Delta A \omega \mu_o}. \tag{24}$$

After inverting the matrix, we then add J_{xn} and J_{yn} to get $\bar{\mathbf{J}}_n(\rho')$. To calculate the far-field RCS, we use the two-dimensional formula,

$$\sigma_{2D} = 2\pi\rho \left(\frac{|\mathbf{H}_{scat}|}{|\mathbf{H}_{inc}|}\right)^2 \tag{25}$$

where the incident H field in free space is $H_{inc} = -(\varepsilon_o/\mu_o)^{1/2} E_{inc}$, and

$$|\mathbf{H}_{scat}| = \left| k \sqrt{\frac{1}{8\pi k\rho}}\, \hat{\rho} \times \left(\sum_{i=1}^{N} \mathbf{J}_i(\rho')\, e^{-ik\rho\cdot\rho'} \Delta A' \right) \right|. \tag{26}$$

Thus, our final equation for the scattering cross section is

$$\sigma_{2\text{-}D}(\phi) = \frac{k\mu_0}{4\epsilon_0}\left(\frac{\Delta A}{E_0}\right)^2 \left| \hat{\rho} \times \sum_{i=1}^{N} J_i e^{ikcos(\phi - \phi_i)\rho_i} \right|^2 . \qquad (27)$$

5. DERIVATION OF SELF-CELL CORRECTION

Until now, we have excluded the entire self-cell as though it were the limiting principal area when, in fact, it may be too large to accurately model a tiny area shrinking in toward the source point at its center. The accuracy improves as the number of cells per wavelength increases, or the relative cell size shrinks. However, this is more and more computationally demanding. As an alternative method for improving the accuracy of our calculation, let us consider first the analogous three-dimensional situation, involving the volumetric self-cell, V_{sc}, surrounding a principal volume, V_δ (see Figure 2). Since we wish to use V_δ instead of V_{sc} for the excluded region, we must calculate the contribution to the total field from the region between V_{sc} and V_δ.

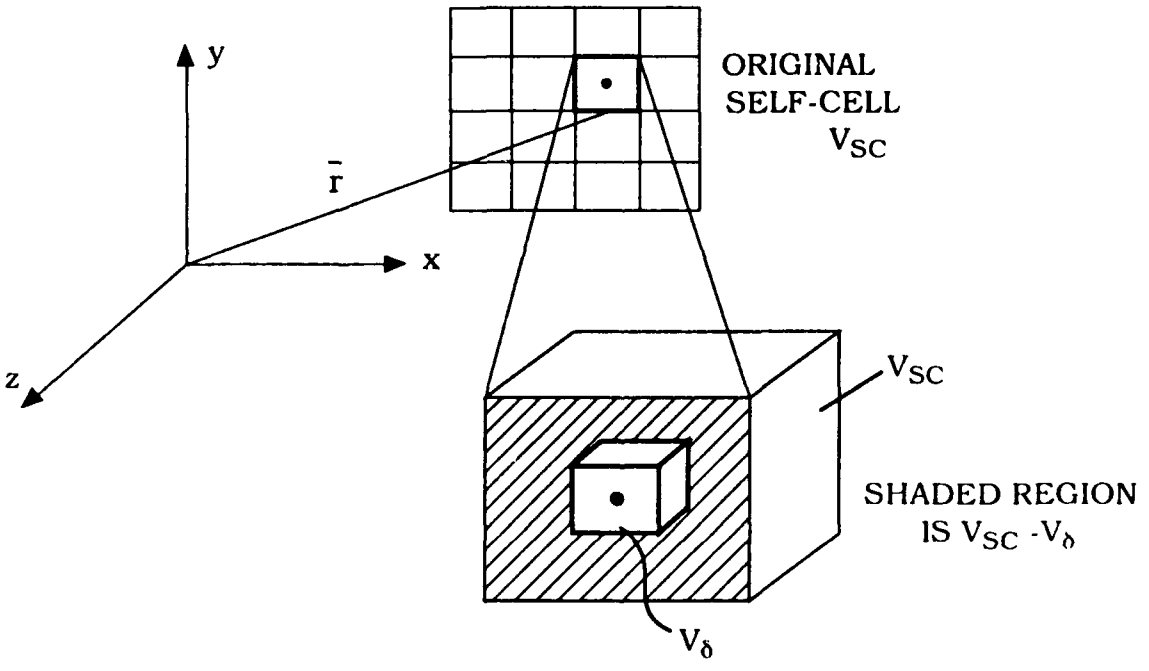

Figure 2. Self-Cell Correction

For these calculations, we will use spheres and circles rather than cubes and squares; conveniently, both shapes have identical principal volume and principal area expressions.[7] The equation we have used until now for the scattered E field excluding an entire self-cell in place of V_δ is

$$\mathbf{E}_{scat}(\mathbf{r}) = i\omega\mu_0 \lim_{\delta\to 0} \int_{V-V_\delta} \bar{\mathbf{G}}_E(\mathbf{r},\mathbf{r}') \cdot \mathbf{J}(\mathbf{r}')\, dV' + \frac{\bar{\mathbf{L}}_\delta \cdot \mathbf{J}(\mathbf{r})}{i\omega\varepsilon_0}. \tag{28}$$

We prefer to use

$$\mathbf{E}(\mathbf{r}) = i\omega\mu_0 \int_{V-V_\infty} \bar{\mathbf{G}} \cdot \mathbf{J}\, dV' + \frac{\bar{\mathbf{L}}_\delta \cdot \mathbf{J}}{i\omega\varepsilon_0} + \Delta\mathbf{E}_{sc-\delta}(\mathbf{r}), \tag{29}$$

where the first term represents the contribution from all the cells, the second term represents the principal volume, and the third term represents the "intermediate" contribution we will proceed to calculate.

Following the ideas outlined by Nachampkin,[7] we formulate $\Delta\mathbf{E}(\mathbf{r})$ as:

$$\Delta\mathbf{E}(\mathbf{r}) = \lim_{\delta\to 0} i\omega\mu_0 \int_{V_{sc}-V_\delta} \bar{\mathbf{G}}_e(\mathbf{r},\mathbf{r}') \cdot \mathbf{J}(\mathbf{r}')\, dV'. \tag{30}$$

Assuming $\mathbf{J}(\mathbf{r}')$ is constant over V_{sc},

$$\Delta\mathbf{E}(\mathbf{r}) = \lim_{\delta\to 0} i\omega\mu_0 \mathbf{J}(\mathbf{r}') \cdot \int_{V_{sc}-V_\delta} \bar{\mathbf{G}}_e(\mathbf{r},\mathbf{r}')\, dV' \tag{31}$$

where

---

[7] Nachampkin, J. (1989) Integrating the dyadic Green's function near sources, *IEEE Transactions on Antennas and Propagation*, **38**:919.

$$\bar{\mathbf{G}}_e = \frac{\nabla \times \nabla \times (\psi \bar{\mathbf{I}})}{4\pi k^2}. \tag{32}$$

We may easily express the electric Green's function in terms of the magnetic Green's function:

$$\bar{\mathbf{G}}_m = \frac{\nabla \times \psi \bar{\mathbf{I}}}{4\pi} = -\frac{1}{4\pi} (\nabla' \times \psi \bar{\mathbf{I}}). \tag{33}$$

Using Stokes' theorem, we then convert the volume integrals into surface integrals:

$$\Delta \mathbf{E}(\mathbf{r}) = \lim_{\delta \to 0} \frac{1}{i\omega\varepsilon_o} \mathbf{J}_{sc} \cdot \left[\int_{S_{sc}} \hat{n}' \times \bar{\mathbf{G}}_m(\mathbf{r}, \mathbf{r}') \, dS' - \int_{S_\delta} \hat{n}' \times \bar{\mathbf{G}}_m(\mathbf{r}, \mathbf{r}') \, dS' \right]. \tag{34}$$

Eliminating $\bar{\mathbf{G}}_m$ from the integrand via

$$\hat{n}' \times \bar{\mathbf{G}}_m = \frac{1}{4\pi} (\hat{n}' \times \nabla\psi \times \bar{\mathbf{I}}) \tag{35}$$

with

$$\nabla\psi = \left(ik - \frac{1}{R} \right) \hat{R} \frac{e^{ikR}}{4\pi R} \tag{36}$$

gives

$$\hat{n}' \times \bar{\mathbf{G}}_m = \frac{(ikR - 1) e^{ikR}}{(4\pi R)^2} [\hat{n}'\hat{R} - (\hat{n}'\cdot\hat{R}) \bar{\mathbf{I}}] . \tag{37}$$

Next, we integrate this quantity over the surfaces S_{sc} and S_δ. If we choose V_{sc} and V_δ to be spheres, where the radius of V_{sc} = a, and that of $V_\delta = r_\delta$, when we integrate over the surface, S_{sc},

the quantity $R = |\mathbf{r} - \mathbf{r}'| = a$, since the observation point is at the center of the sphere. V_{sc}, and the source points, $\mathbf{r}'$ are on its surface (see Figure 3). Likewise, when we integrate over the surface S_δ, $R = r_\delta$.

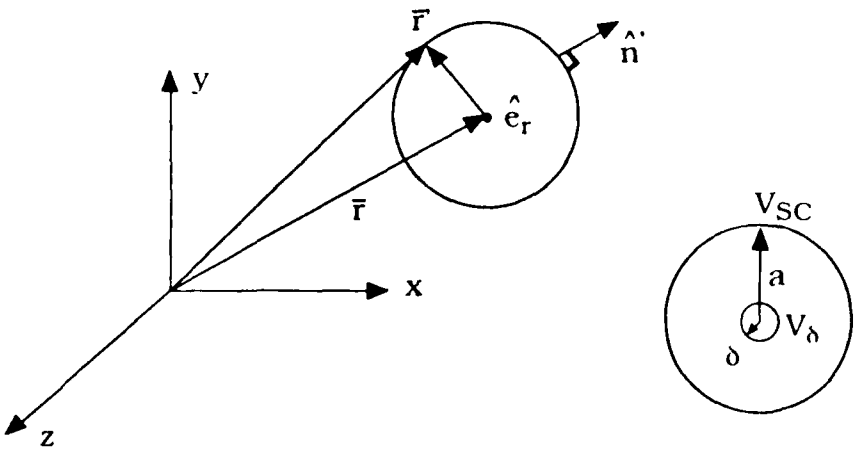

Figure 3. Principal Volume Relative to Volume of Self-Cell

$$\int_{S_{sc}} \hat{n}' \times \bar{G}_m(\mathbf{r}, \mathbf{r}')\, dS' = \frac{1}{4\pi}(ika-1)\, e^{ika}\left[\frac{1}{4\pi}\int_{S_{sc}} -\frac{\hat{n}'\hat{e}_r}{a^2}\, dS' + \frac{1}{4\pi}\int_{S_{sc}} \frac{\bar{I}}{a^2}\, dS'\right]. \tag{38}$$

We recognize the term

$$\frac{1}{4\pi}\int_{S_{sc}} \frac{\hat{n}'\hat{e}_r}{a^2}\, dS' \tag{39}$$

as the definition of $\mathbf{L}_{sc}$[5], and since $\bar{I}$ is constant, the second integral reduces to $\mathbf{I}$. Thus,

$$\int_{S_{sc}} \hat{n}' \times \bar{G}_m(\mathbf{r}, \mathbf{r}')\, dS' = \frac{1}{4\pi}(ika-1)\, e^{ika}\,[-\bar{L}_{sc} + \bar{I}]\,. \tag{40}$$

Analogously, with r_δ as the radius of V_δ.

$$\int_{S_\delta} \hat{n}' \times \bar{G}_m(\mathbf{r}, \mathbf{r}')\, dS' = \frac{1}{4\pi} (ikr_\delta - 1)\, e^{ikr_\delta} [-\bar{L}_\delta + \bar{I}]. \tag{41}$$

So, our equation for the intermediate electric field becomes

$$\Delta \mathbf{E}(\mathbf{r}) = \lim_{\delta \to 0} \frac{1}{4\pi i\omega\varepsilon_o} \mathbf{J}_{sc} \cdot \{ (ika - 1)\, e^{ika} [-\bar{L}_{sc} + \bar{I}] - (ikr_\delta - 1)\, e^{ikr_\delta} [-\bar{L}_\delta + \bar{I}] \}. \tag{42}$$

Taking the limit as $\delta \to 0$, so $r_\delta \to 0$, and considering the source dyadic for a sphere,

$$\bar{L}_\delta = \bar{L}_{sc} = \frac{\bar{I}}{3}. \tag{43}$$

We now have:

$$\Delta \mathbf{E}(\mathbf{r}) = \frac{\mathbf{J}_{sc}}{6\pi i\omega\varepsilon_o} \{ (ika - 1)e^{ika} + 1 \}. \tag{44}$$

Now, we solve the two-dimensional problem in a completely analogous manner, using a circular self-cell and circular principal area. For the TM polarization, we had the equation for the scattered electric field,

$$\mathbf{E}_z(t) = i\omega\mu_o \int_{A - A_{sc}} [\bar{g}^o_c(t, t') \cdot \mathbf{J}(t')]_z\, dA' + \Delta \mathbf{E}_z(t). \tag{45}$$

To develop an expression for the intermediate field, we once again assume the current is constant over the area of the self-cell.

$$\Delta \mathbf{E}_z(\mathbf{t}) = \lim_{\delta \to 0} J_z \, i\omega\mu_o \int_{A_{sc}-A_\delta} \bar{\mathbf{g}}^o_{zz} \, dA', \tag{46}$$

and express the Green's function in terms of the Hankel function in the integrand:

$$\Delta \mathbf{E}_z(\mathbf{t}) = \frac{-\omega\mu_o}{4} J_z \lim_{\delta \to 0} \int_{A_{sc}-A_\delta} H_o^{(1)}(k\rho) \, dA'. \tag{47}$$

We can solve the indefinite integral:

$$\int H_o^{(1)}(k|\mathbf{t} - \mathbf{t}'|) \, dA' = \frac{2\pi\rho}{k} H_1^{(1)}(k\rho). \tag{48}$$

If we put in the limits ρ_δ and a, we have our result --

$$\Delta E_z(\mathbf{t}) = \frac{-\omega\mu_o\pi}{2k} J_z \lim_{\delta \to 0} [aH_1^{(1)}(ka) - \rho_\delta H_1^{(1)}(k\rho_\delta)]. \tag{49}$$

Continuing with the TE polarization, we had the equation for the scattered field:

$$\mathbf{E}(\mathbf{t}) = i\omega\mu_o \int_{A-A_{sc}} \bar{\mathbf{g}}^o_e(\mathbf{t}, \mathbf{t}') \cdot \mathbf{J}(\mathbf{t}') \, dA' + \frac{\mathbf{J}_t(\mathbf{t})}{2i\omega\varepsilon_o} + \Delta\mathbf{E}(\mathbf{t}), \tag{50}$$

and

$$\Delta\mathbf{E}(\mathbf{t}) = i\omega\mu_o \lim_{\delta \to 0} \int_{A_{sc}-A_\delta} \frac{i}{4k^2} (\nabla_t \times \nabla_t \times H_o^{(1)} \bar{\mathbf{I}}) \cdot \mathbf{J}_t \, dA', \tag{51}$$

just as in the three-dimensional case. Next, we write $\Delta\mathbf{E}$ in terms of $\bar{\mathbf{g}}^o_m$, assuming $\mathbf{J}_t$ is constant over A_{sc}

$$\Delta \mathbf{E}(t) = \frac{1}{\omega \varepsilon_o} \mathbf{J}_t \bullet \left[\int_{A_\infty} (\nabla_t \times \bar{\mathbf{g}}_m^o) \; dA' \; - \lim_{\delta \to 0} \int_{A_\delta} (\nabla_t \times \bar{\mathbf{g}}_m^o) \; dA' \right]. \tag{52}$$

Since we can also show

$$\int_A (\nabla_t \times \mathbf{A}) \, dA = \int_C (\hat{n}_t \times \mathbf{A}) \, dC, \tag{53}$$

we apply this two-dimensional version of Stokes' theorem to the two area integrals in Eq. (52), to get

$$\Delta \mathbf{E}(t) = \frac{1}{\omega \varepsilon_o} \mathbf{J}_t \bullet \left[\int_{C_\infty} (\hat{n}' \times \bar{\mathbf{g}}_m^o) \, dC' - \lim_{\delta \to 0} \int_{C_\delta} (\hat{n}' \times \bar{\mathbf{g}}_m^o) \; dC' \right]. \tag{54}$$

Substituting Hankel functions for the cross product in this case gives

$$\hat{n}' \times \bar{\mathbf{g}}_m^o = \frac{i}{4} [\hat{n}_t \nabla_t H_o^{(1)} - (\hat{n}_t \cdot \nabla_t H_o^{(1)}) \, \bar{I}]. \tag{55}$$

The gradient of the Hankel function comes out to be

$$\nabla_t H_o^{(1)} = \frac{(t - t')}{|t - t'|} k H_1^{(1)} \equiv -\hat{e}_t k H_1^{(1)}, \tag{56}$$

so

$$\hat{n}_t \times \bar{\mathbf{g}}_m^o = \frac{ik}{4} H_1^{(1)} [\bar{I} - \hat{n}_t \hat{e}_t], \tag{57}$$

and substituting back into the contour integrals,

$$\Delta\mathbf{E}(t) = \frac{-k}{4\omega\varepsilon_0}\,\mathbf{J}_t \cdot \left[H_1^{(1)} \int_{C_{sc}} (-\hat{n}_t \hat{e}_t + \bar{\mathbf{I}})\, dC' - \lim_{\delta \to 0} H_1^{(1)} \int_{C_\delta} (-\hat{n}_t \hat{e}_t + \bar{\mathbf{I}})\, dC' \right]. \tag{58}$$

Note that the Hankel function is constant over the perimeter contours, as we evaluate the four integrals around the circles C_{sc} and C_δ, with the radius of C_{sc} = a, and that of $C_\delta = \rho_\delta$. $\bar{\mathbf{I}}$ is also constant, and we recognize

$$\int_{C_\delta} \frac{\hat{n}_t \hat{e}_t}{2\pi T'}\, dC' = \bar{\mathbf{I}}_\delta. \tag{59}$$

For a circle, we use[5]

$$\bar{I}_\delta = \bar{I}_{sc} = \frac{\bar{\mathbf{I}}}{2}, \tag{60}$$

and our result becomes

$$\Delta\mathbf{E}(t) = \frac{-\omega\mu_0\pi}{4k}\,\mathbf{J}_t \left[a\, H_1^{(1)}(ka) - \lim_{\delta \to 0} \rho_\delta\, H_1^{(1)}(k\rho_\delta) \right]. \tag{61}$$

This is quite similar to the result for the TM polarization. For the last term, we can use the small argument approximation for the Neumann function to get

$$\lim_{\delta \to 0} \; -i\rho_\delta \frac{1}{\pi}\, \Gamma(1) \left(\frac{1}{2}\, k\rho_\delta \right)^{-1}. \tag{62}$$

The gamma function evaluates to unity, giving us the value

$$-\frac{2i}{\pi k} \tag{63}$$

for the desired limit. Substituting this into our results for both two-dimensional polarizations we have:

$$\Delta E_z(t) = \frac{-\omega\mu_o\pi}{2k} J_z \left[a H_1^{(1)}(ka) + \frac{2i}{\pi k} \right]. \tag{64}$$

and

$$\Delta \mathbf{E}(t) = \frac{-\omega\mu_o\pi}{4k} \mathbf{J}_t \left[a H_1^{(1)}(ka) + \frac{2i}{\pi k} \right]. \tag{65}$$

In the numerical calculation we simply replace the circular principal area with an equivalent square principal area by forcing $s = \pi^{1/2}a$, or in the case of volumes in three dimensions, $s = (4/3\,\pi)^{1/3}a$.

6. NUMERICAL CALCULATION OF SCATTERING CROSS SECTION

Once we have arrived at the matrix equation, we simply choose a matrix solution method to calculate the vector **x** in **Ax** = **B**, corresponding to the current induced in the target. Recall also that **B** is the incident field vector, and the matrix **A** consists of Hankel functions that depend only on the distances between the source and observation points. We initially chose a Gauss-Seidel routine to invert the matrix, but recommend the conjugate gradient method be used in a continuation of this project.[6] The program discussed in this report works only for a rectangular cylinder divided evenly into square patches, but can be modified for alternative geometries; the analytical equations hold for an arbitrarily-shaped scatterer. It might be a useful exercise to modify the code so it will accommodate a circular cylinder, since a closed form solution exists for comparison with that particular case, although the physical optics standard is thought to be a sufficiently accurate basis for comparison.

Figure 4 shows the model on which the code is based. A plane wave (at left) is incident on the infinite rectangular cylinder, and the bistatic RCS is calculated as a function of the angle ϕ as indicated. The cross-sectional area of the cylinder is divided evenly into square patches, indexed according to Figure 5, to take advantage of the rectangular symmetry. The origin of the coordinate system is always set up to be at the geometric center of the target. The target dimensions are specified on input and the program adjusts the incident field vector accordingly if the polarization is specified as TE. The program expects either a square or a

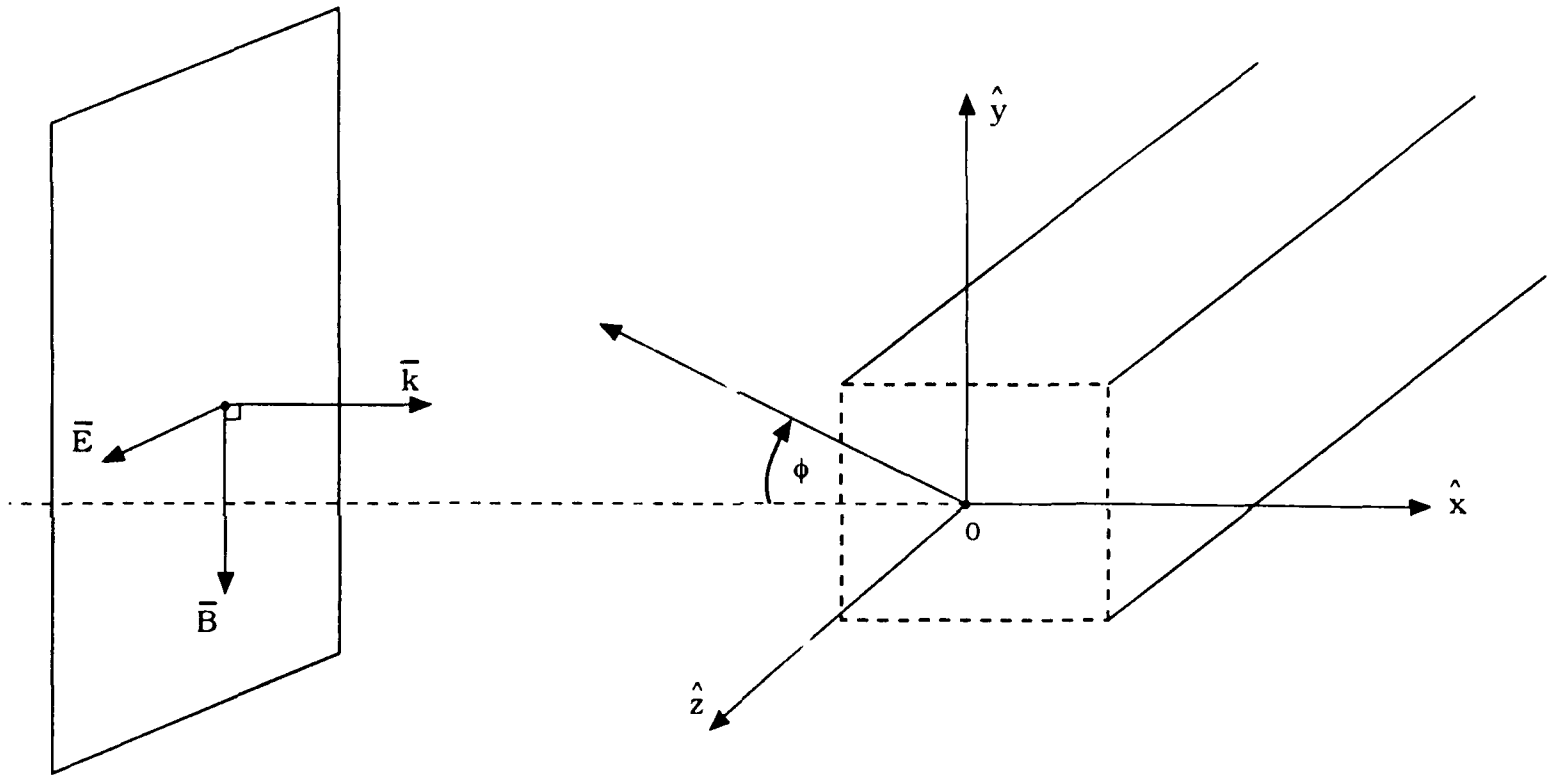

$$\bar{E}_{inc} = \hat{z}\, E_z = \hat{z}\, E_o\, e^{ikx}$$

$$\sigma_{2\text{-}D} = 2\pi\rho \left(\frac{|\bar{H}_{scat}|}{|\bar{H}_{inc}|} \right)^2$$

Figure 4. RCS Model Used in Code

vertical target that is, with the longest side in the y-direction. The z-dimension is infinite for a two-dimensional problem. The incident wave vector points in the +x-direction. The program checks to make sure the user specified a vertical target. If the user inputs a horizontal target, the program rotates the target and sets the incident wave vector in the +y-direction, for grazing incidence. Thus, the user defines the two cases of plane-wave incidence by the order in which the dimensions of the *target* appear in the input file.

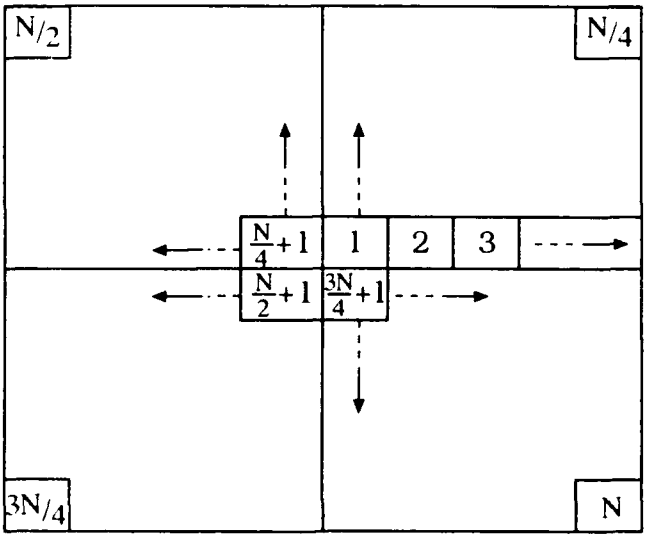

Figure 5. Indexing Scheme for a Rectangular Target Divided Evenly Into Square Patches

Results were obtained for a variety of targets. Initial test runs were made with a square cylinder, 0.8 x 0.8 wavelength, for z-polarization, for several values of the ratio ϵ/ϵ_0. When this ratio was set to 3.0, runs were made for N = 4, 16, 64, and 100. Results for these runs appear in Figures 6 and 7. The ratio was then set to 1.1 to simulate a target that was almost invisible to the wave (free-space target), to make sure the RCS approached zero. Figure 8 verifies this limit. The run time for a target with 100 patches (N = 100) was about 10 minutes.

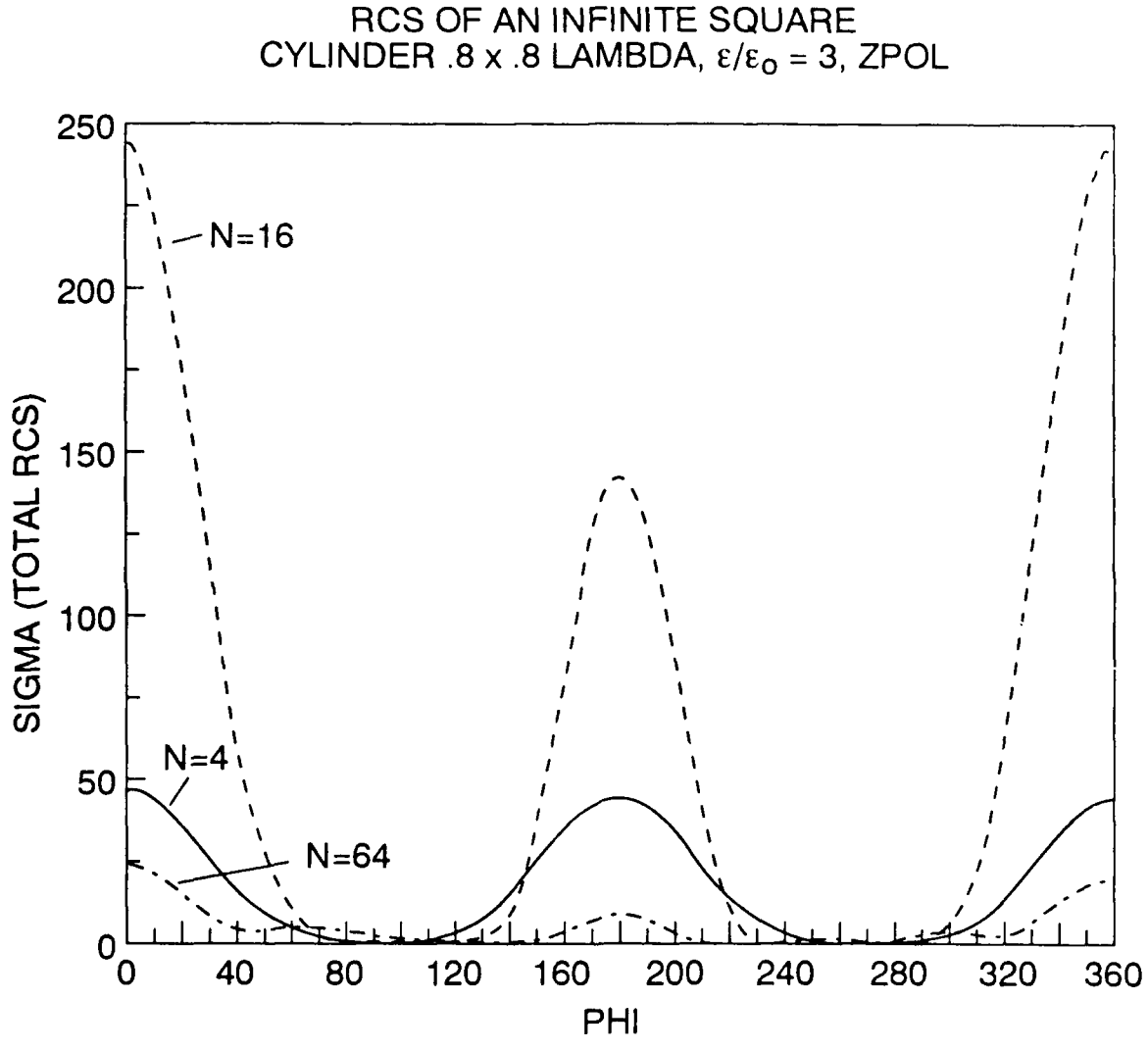

Figure 6. RCS of an Infinite Square Cylinder, 0.8 x 0.8 λ, $\varepsilon/\varepsilon_0 = 3$, Z Polarization, N = 4, 16, and 64

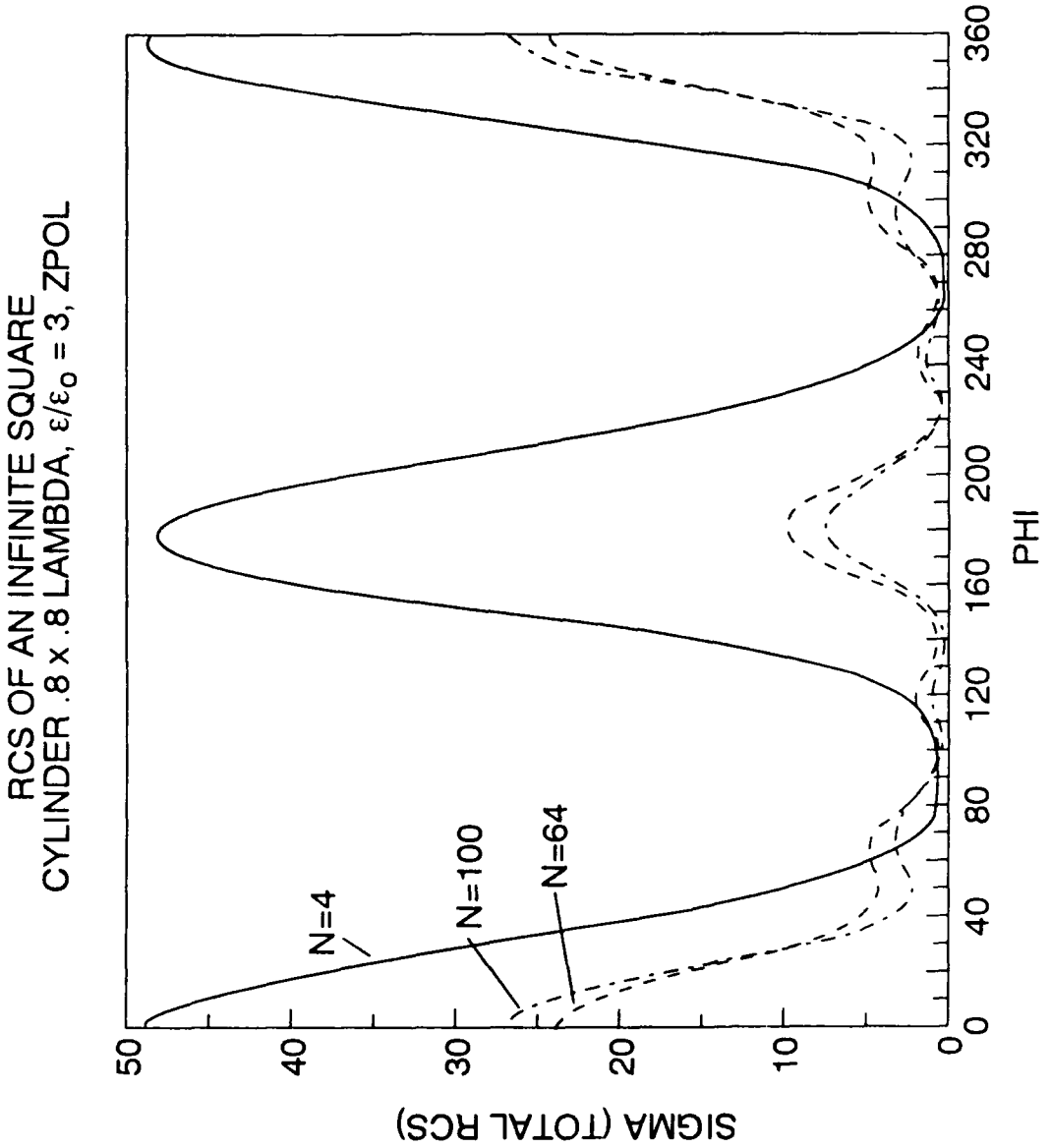

Figure 7. RCS of an Infinite Square Cylinder, 0.8 x 0.8 λ, $\varepsilon/\varepsilon_0 = 3$. z Polarization. N = 4, 64, and 100

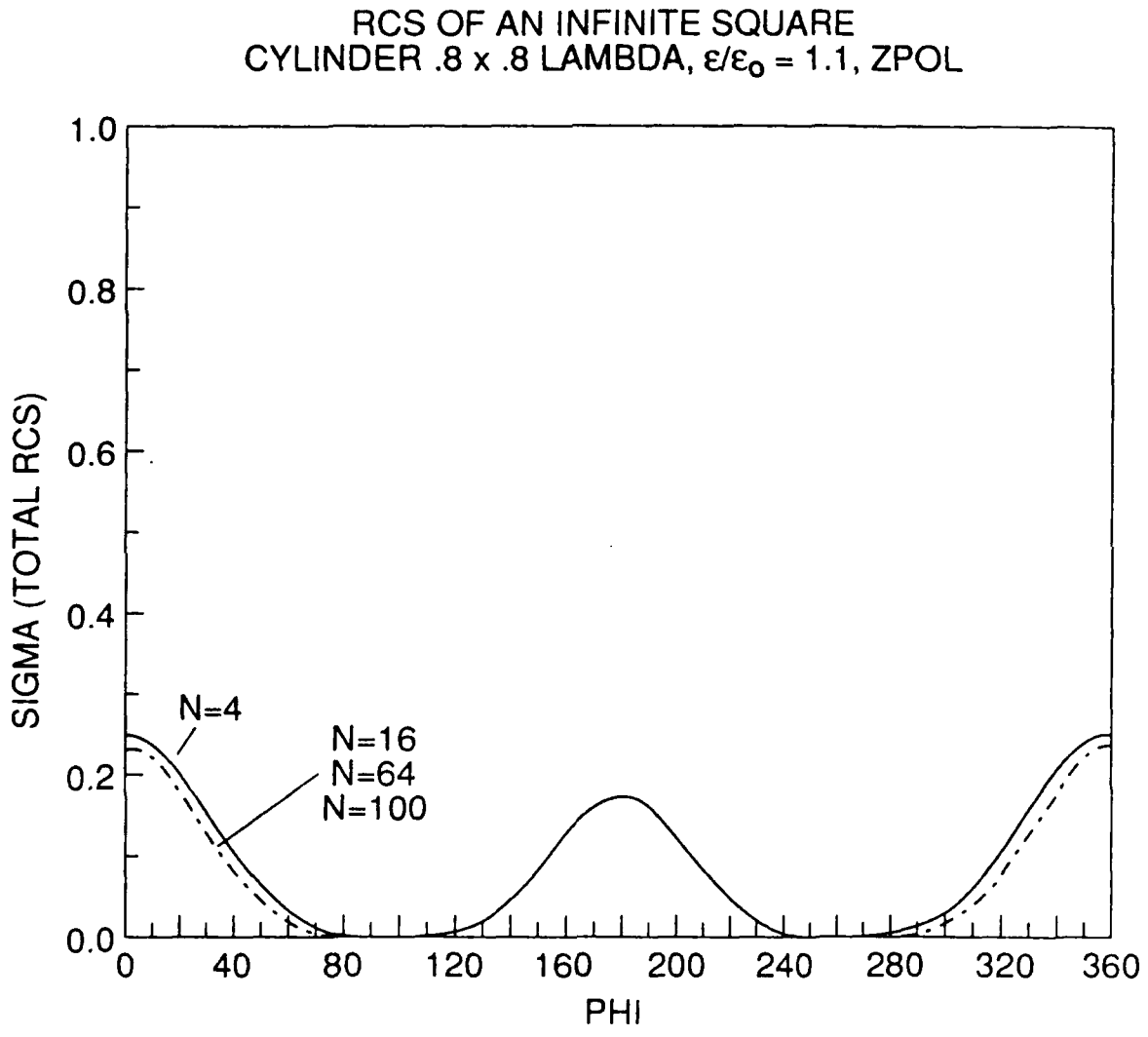

Figure 8. RCS of an Infinite Square Cylinder, 0.8 x 0.8 λ, $\varepsilon/\varepsilon_0 = 1.1$, Z Polarization

The next set of runs, at the top of Figure 9, also had a z-polarized incident wave, but the parameters were set to correspond to Richmond's example (bottom). Richmond[3] used an epsilon ratio of 4.0 and a slab measuring 50 patches x 1 and 2.5 x 0.05 wavelengths. We used a similar slab measuring 100 patches x 2, but the real dimensions are still 2.5 x 0.05 wavelengths. Since we have 4 times as many patches, we expect an improvement in accuracy. We ran both orientations with respect to the incident wave, as he did. We refer to these as "horizontal target" (grazing incidence) and "vertical target", (normal incidence) and they are depicted in the two columns of Figure 9. (Although we use $\phi = 0$ as backscatter and 180° as the forward scatter direction our angles in Figures 9 and 10 have been shifted to conform to Richmond's definition.) Figure 10 shows the corresponding results for the xy- or TE polarization. All the results of Figures 9 and 10 include the self-cell correction.

The graphs are identical for z-polarization, with a horizontal target. For both polarizations, the vertical target graph is closer to the physical optics approximation than is Richmond's. The horizontal target RCS for the xy-polarization is slightly higher than Richmond's, but he gives no physical optics result for comparison in this case.

We experimented with leaving out the $\bar{\mathbf{L}} \cdot \mathbf{J}$ source term for the TE case, and found that as expected, the $\bar{\mathbf{L}} \cdot \mathbf{J}$ term is necessary to achieve a correct result. The self cell correction then fine-tunes the accuracy of the RCS. We have presented a complete development of the theory leading to this calculation, where Richmond omits this issue from his discussion, or incorporates the information contained in these terms by some other means. All the data were produced using either the VAX 11-750 at RADC/EECT or the VAX 8650 scientific machine at AFGL.

7. FUTURE EXTENSIONS

The original intent of this project was to continue, and to solve the problem in three dimensions as well, and to allow for an inhomogeneous target (where μ and ϵ vary with position). The three-dimensional problem will involve inverting a matrix with N proportional to $(d/\lambda)^3$ rather than $(d/\lambda)^2$ for two dimensions. Although it has been said that the analytical calculation is less cumbersome than what we have already done for the two-dimensional case, the computer resources needed are significantly greater.

Following are some suggestions for decreasing the computing time. First, one should use a more efficient matrix solver, (such as conjugate gradient iteration combined with the FFT), and consider the advantage of using dimensionless variables in the code, which also simplifies the process of varying parameters. Furthermore, this problem, especially the inhomogenous form, is a good candidate for a parallel processor. It might also be interesting to consider doing a timestepped simulation of wave scattering, as an alternative to using the computer in its usual number-crunching role.

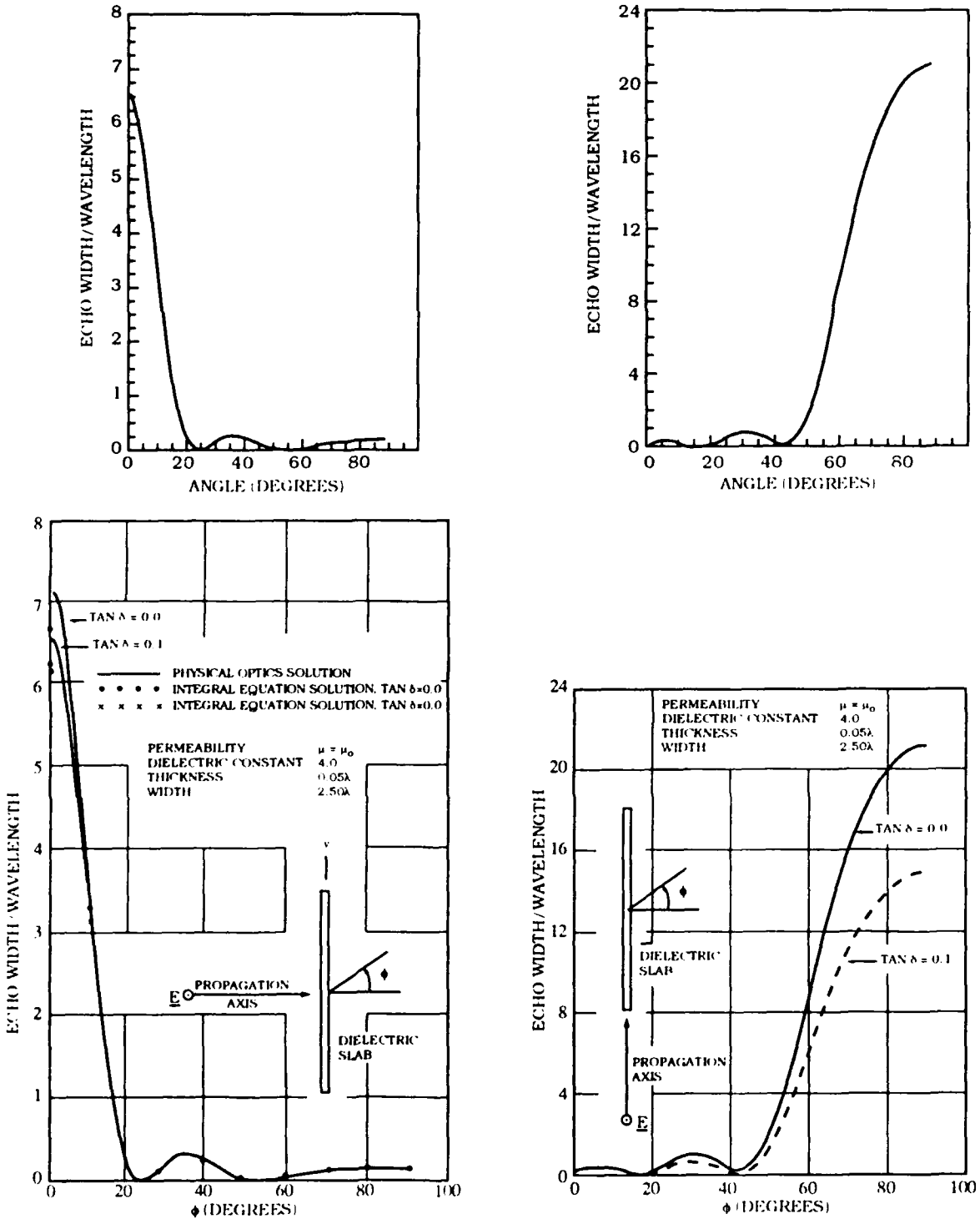

Figure 9. Upper left: RCS of an Infinite Square Cylinder, 0.05 x 2.50 λ, ϵ/ϵ_0 = 4.0, Z Polarization, With Vertical Target. Upper right: with horizontal target; for comparison with upper left. Lower left: calculated scattering patterns of a homogeneous plane dielectric slab of the same thickness and width as above, with a plane wave having normal incidence, and lower right: with a plane wave at grazing incidence [after Richmond]

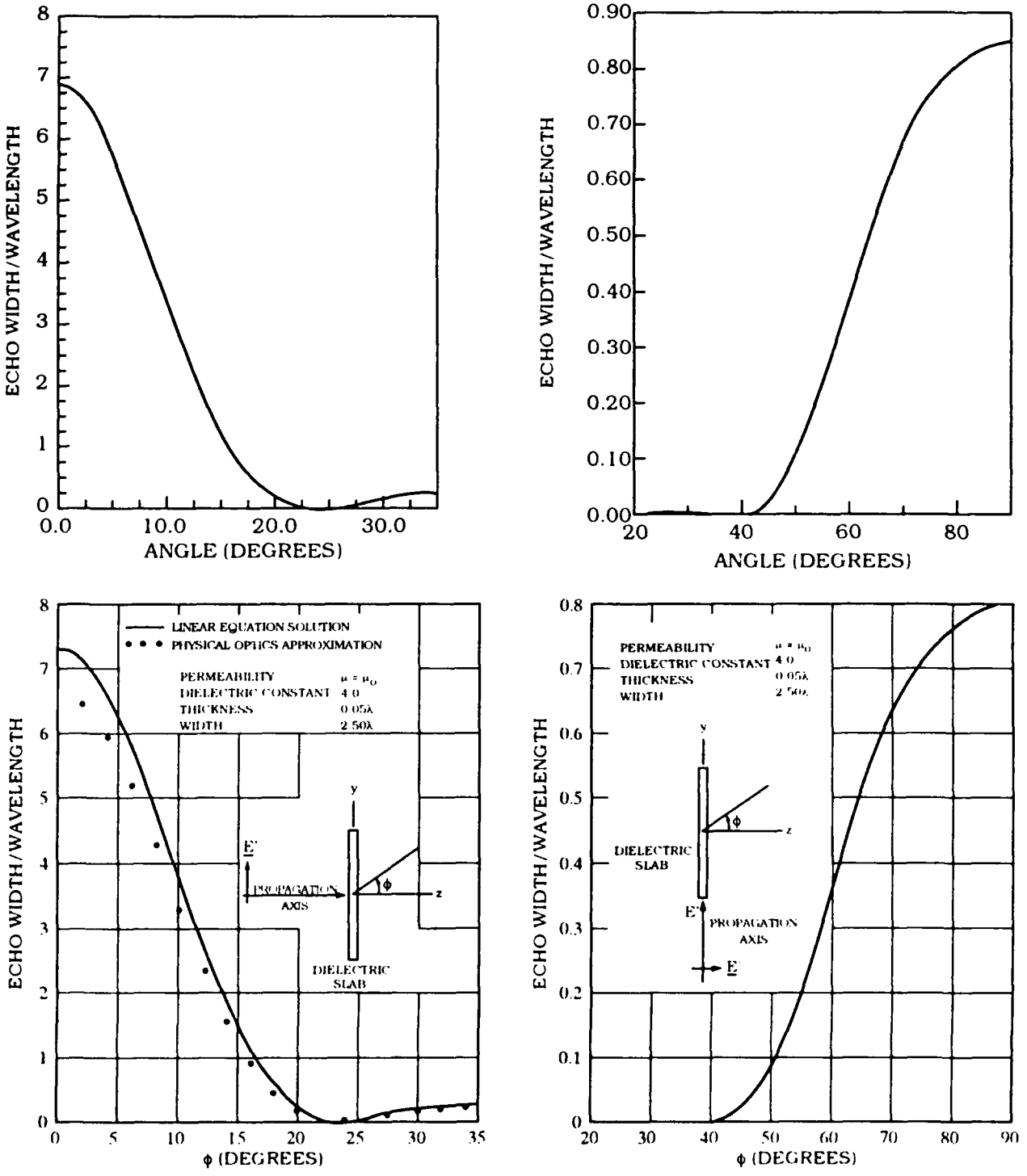

Figure 10. Same as Figure 9, but for xy, or TE Polarization